ELSEVIER

Journal of Alloys and Compounds 224 (1995) 316–329

Journal of ALLOYS AND COMPOUNDS

Description of the Cu–As–Se ternary system

Kamira Cohen, Jacques Rivet, Jérôme Dugué

Laboratoire de Chimie minérale structurale, Faculté des sciences pharmaceutiques et biologiques, Université René Descartes, 4 avenue de l'Observatoire, 75270 Paris Cedex 06, France

Received 22 August 1994; in final form 2 January 1995

Abstract

The phase diagram of the Cu–As–Se ternary system was studied by differential thermal analysis, X-ray diffraction and metallography analysis. Two ternary phases are observed: the Cu_3AsSe_4 compound, which melts congruently, and the $CuAsSe_2$ compound, which undergoes a peritectic decomposition. The ternary system is subdivided into 12 secondary triangles. The 12 ternary invariants are localized: six eutectics, one of which is degenerated at the selenium apex, and six peritectics. Two ternary liquid–liquid miscibility gaps originating from the Cu–Se binary system are identified. One of these is crossed by a eutectic valley giving a first-class ternary monotectic equilibrium. A large vitreous region, which comes from the As–Se binary glass zone, is identified; it overlaps the liquid–liquid miscibility area, giving phase-separated glasses.

Keywords: Phase diagrams; Glassy domain; Liquid–liquid miscibility gap; Binary systems; Ternary systems

1. Introduction

This study has been performed on the ternary Cu–As–Se system to determine the composition of the different crystalline phases, the area of the glassy domain and some electrical properties of the glasses. The few studies performed have been concentrated on defining the boundaries of the glassy area and the electrical properties along the section $Cu_x(As_2Se_3)_{1-x}$.

No thermal study has been thoroughly realized on this subject. Therefore, we found it interesting to specify the crossings of the eutectic valleys, the compositions of the ternary invariants, and the domains of the two liquid–liquid miscibility gaps originating from the Cu–Se binary system. In this study we confirm the existence of the two ternary phases Cu_3AsSe_4 and $CuAsSe_2$. However, we cannot prove the existence of the compound CuAsSe. The congruently melting compound Cu_3AsSe_4 has been described with the tetragonal famatinite type, connected to the blende structure. The second compound, $CuAsSe_2$, crystallizes in the cubic sphalerite type and undergoes a binary peritectic decomposition. Liang et al. [1] give the temperature of the melting points and the X-ray diffraction patterns of these two compounds. By using EXAFS (extended X-ray absorption fine structure) Hunter [2] has studied the atomic coordination in the crystalline and glassy forms of the compound $CuAsSe_2$.

2. Materials and methods

The Cu–As–Se ternary system was studied by differential thermal analysis, X-ray diffraction and metallography analysis.

The differential thermal analyzer (DTA) included a furnace and a Netzsch autotimer associated to a Linseis recorder. The thermocouples used were made of Pt–Pt (10% Rh). The heating rate was 10 °C min^{-1}. The analyzer was standardized by the elements Sn: $T_f = 232$ °C, Sb: $T_f = 631$ °C and Ag: $T_f = 962$ °C.

X-ray diffraction studies were performed by a Guinier–de Wolff camera. Some of the samples were also examined by a Guinier–Lenné camera while heating the sample.

The syntheses of the samples (Fig. 1) were carried out in an evacuated (10^{-3} Torr) quartz ampoule using elements of high-purity grade (99.999%). As arsenic oxidizes rapidly it was purified by sublimation at 280 °C in a silica ampoule before use. All the preparations weighed approximately 600 mg so that the different DTA thermograms could easily be compared. To avoid evaporation and condensation of selenium at the apex of the ampoule, the samples were slowly heated. The samples were kept at 800 °C for about 48 h to insure a homogeneous melt. They were then either slowly cooled or quenched in cold water.

SSDI 0925-8388(95)01534-5

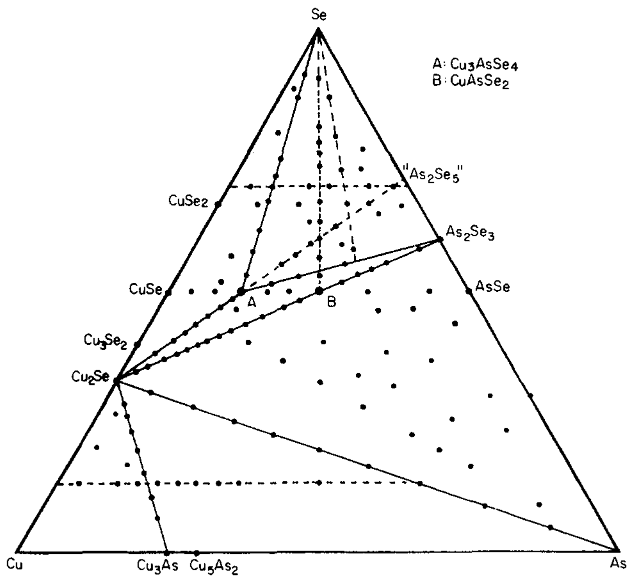

Fig. 1. Compositions studied in the Cu–As–Se ternary system.

The liquid–liquid miscibility gap originating from the Cu–Cu_2Se binary system shows a monotectic isothermal line at 1107 °C; it partly extends into the ternary system. Samples with compositions found in this region were heated in a Hermann–Morritz furnace at 1180 °C and then quenched in cold water. The block samples were included in a resin and were successively polished by abrasive papers made of silicon carbide with decreasing size. The last step of polishing was performed by the use of abrasive suspensions held on Struers disks. The surfaces of the specimens were examined by a metallographic microscope.

3. Bibliographic data on the binary systems

We have studied the constituent binary systems of the ternary system. Our results generally agree with the bibliographic data, which we give below, to be used in the construction of the ternary diagram.

3.1. *The Cu–As binary system*

As arsenic is highly volatile, this binary system, studied by Hume-Rothery and Burns [3], is not described in its entirety. In fact, arsenic condenses at the upper part of the ampoule, giving an important deviation from stoichiometry. The Cu–As system includes several phases:

(1) The Cu_3As phase shows a congruent melting at 827 °C. Heyding and Despault [4] confined their study to a domain of miscibility between the compositions 25 and 27 at.% As. The lattice parameters of this phase, which crystallizes in the hexagonal system, decrease as the As content increases:

$a=7.132$ Å, $c=7.304$ Å at 25 at.% As

$a=7.113$ Å, $c=7.272$ Å at 27 at.% As

(2) An incongruently melting phase, Cu_5As_2, was found to be stable in the interval from 395 to 710 °C. The reaction of decomposition is:

$Cu_5As_2 \rightleftharpoons Cu_3As + \text{Liq. } p_1$

The tetragonal lattice parameters of Cu_5As_2 are:

$a=7.48$ Å, $c=7.12$ Å with $c/a=0.95$

(3) A third phase is proposed by Heyding and Despault [4] and by Schubert et al. [5]. However, these authors disagree about the stoichiometry and the lattice parameters. Heyding and Despault [4] suggest the Cu_8As formula with a hexagonal structure and with the lattice parameters as:

$a=2.558\pm0.001$ Å, $c=4.226\pm0.001$ Å

Schubert et al. [5] also consider a hexagonal lattice but with the stoichiometry of Cu_9As and with the lattice parameters as:

$a=2.60$ Å, $c=4.26$ Å with $c/a=1.64$

According to the study presented by Hawkins [6], the highest melting point does not correspond to the Cu_3As formula but rather to $Cu_{73.7}As_{26.3}$. The phase diagram of the Cu–As system presents two miscibility zones. The first one extends from Cu_3As to 27.55 at.% As and the second one is found in the area near Cu. On both sides of Cu_3As a eutectic appears: the first one, e_2, with a composition equal to 18.4 at.% As and the second one, e_3, with a composition of 46 at.% As at the temperatures of 685 °C and 600 °C respectively.

Our study confirms earlier results; however, we observed some slight discrepancies in temperature and composition values. The peritectoid decomposition of the Cu_8As compound is shown as a small endothermic peak at 380 °C. The Cu_5As_2 phase is stable between 395 °C and 710 °C. Both binary eutectics appear at about the temperatures given by Hume-Rothery and Burns [3]. Fig. 2 presents the Cu–As binary system according to our results. Table 1 gives the phase equilibria (formulas of phases written in parentheses correspond to solid miscibility domains).

3.2. *The Cu–Se binary system*

Friedrich and Leroux [7] studied the Cu–Se system up to 40 at.% Se. Heyding [8] completed this work up to 70 at.% Se. The phase diagram contains several phases. Table 2 shows the lattice parameters of the different crystalline phases.

The Cu_2Se compound undergoes a polymorphic transformation at 131–135 °C and congruently melts at

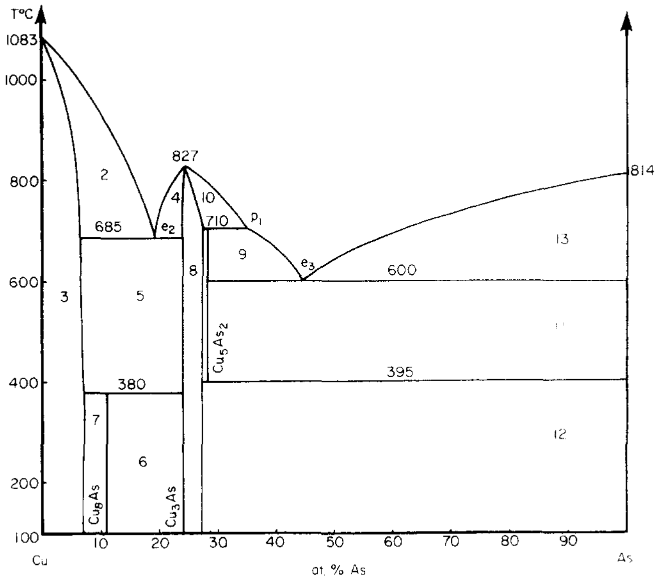

Fig. 2. Phase diagram of the Cu–As binary system.

Table 1
Phase equilibria in the Cu–As binary system

Domain number	Phases
1	L
2	L+(Cu)
3	(Cu)
4	$L+Cu_3As$
5	$(Cu)+Cu_3As$
6	Cu_8As+Cu_3As
7	$(Cu)+Cu_8As$
8	(Cu_3As)
9	$L+Cu_5As_2$
10	$L+(Cu_3As)$
11	Cu_5As_2+As
12	$(Cu_3As)+As$
13	L+As

1148 °C. The $Cu_{2-x}Se$ solid solution extends from 33 to 38 at.% Se. This miscibility domain presents its maximal extension at 380 °C. The Cu_3Se_2 compound undergoes a peritectoid decomposition at 135 °C according to the equation:

$$Cu_3Se_2 \rightleftharpoons (Cu_2Se)+CuSe$$

Two other binary phases exist in this system, namely CuSe and $CuSe_2$. Both show incongruent melting and decompose according to the reactions:

$$CuSe \rightleftharpoons (Cu_2Se)+\text{Liq. } p_3 \quad \text{at } 380\ °C$$

$$CuSe_2 \rightleftharpoons CuSe+\text{Liq. } p_4 \quad \text{at } 334\ °C$$

By using DTA a polymorphic transformation of the CuSe compound is observed at 50 °C. The $Cu_{2-x}Se$ solid solution divides the Cu–Se diagram into two independent parts, each containing a two-liquid miscibility gap:

(1) The first one is found in the $Cu–Cu_2Se$ domain and presents an isothermal monotectic line at 1107 °C; the extension of this miscibility gap is relatively small (between 6 and 32 at.% Se).
(2) The second one is found in the CuSe–Se domain and shows an isothermal monotectic line at a lower temperature of about 528 °C. This two-liquid miscibility gap extends largely from 53.5 to 95 at.% Se.

Our study (Fig. 3) confirms the results presented by Heyding [8]. Table 3 gives the phase equilibria of the Cu–Se system.

3.3. The As–Se binary system

The As–Se diagram has been described by several authors. Dembovskii and Luzhnaya [9] observed the presence of two intermediate compounds, As_2Se_3 and As_4Se_4, which congruently melt at 360 °C and 280 °C respectively. According to Myers and Felty [10] only As_2Se_3 congruently melts at 375 °C whereas As_4Se_4 undergoes a peritectic decomposition at 270 °C corresponding to the equilibrium:

$$As_4Se_4 \rightleftharpoons As_2Se_3+\text{Liq. } p_2$$

On both sides of the two compounds a eutectic appears: at 250 °C, e_4 with a composition equal to 55 at.% As and, at 154 °C, e_5 with a composition equal to 20 at.% As.

Table 2
Crystallographic data in the Cu–Se binary system

Composition	System	Space group	*a* (Å)	*b* (Å)	*c* (Å)
$Cu_{1.84}Se$	Cubic	*Fm3m*	5.764 ± 0.001	–	–
$Cu_{1.80}Se$	Cubic	*Fm3m*	5.759 ± 0.001	–	–
$Cu_{1.70}Se$	Cubic	*Fm3m*	5.743 ± 0.002	–	–
Cu_3Se_2	Tetragonal	*P4/mmm*	6.394 ± 0.005	–	4.269 ± 0.005
αCuSe	Hexagonal	*P6₃/mmc*	3.940 ± 0.003	–	17.216 ± 0.005
βCuSe	Orthorhombic	–	6.81 ± 0.01	4.01 ± 0.01	17.09 ± 0.02
$CuSe_2$	Orthorhombic	*Pnnm*	5.01 ± 0.01	6.19 ± 0.01	3.741 ± 0.005

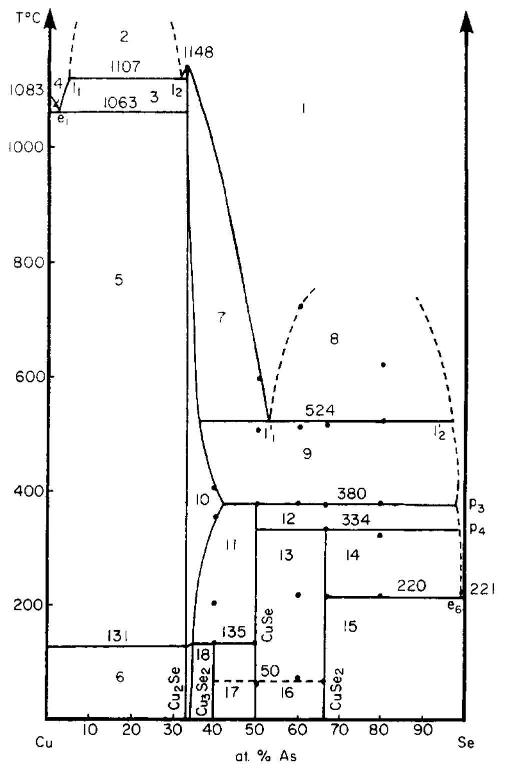

Fig. 3. Phase diagram of the Cu–Se binary system.

Table 3
Phase equilibria in the Cu–Se binary system

Domain number	Phases
1	L
2	L_1+L_2
3	$L_2+Cu_2Se\beta$
4	L_1+Cu
5	$Cu+(Cu_2Se\beta)$
6	$Cu+(Cu_2Se\alpha)$
7	$L'_1+(Cu_2Se\beta)$
8	$L'_1+L'_2$
9	$L'_2+Cu_2Se\beta$
10	$(Cu_2Se\beta)$
11	$(Cu_2Se\beta)+CuSe\beta$
12	$L'_2+CuSe\beta$
13	$CuSe\beta+CuSe_2$
14	L'_2+CuSe_2
15	$CuSe_2+Se$
16	$CuSe\alpha+CuSe_2$
17	$Cu_3Se_2+CuSe\alpha$
18	$(Cu_2Se\alpha)+Cu_3Se_2$

Blachnik et al. [11] admit the results of Myers and Felty [10], and moreover consider the existence of another compound, namely As_4Se_3. However, they give no precise conditions on its fusion. Rouland [12] lends support to the preceding results and confirms the As_4Se_3 compound already described by Bastow and Whitfield [13]. Our results do not prove the existence of this compound. The reason for this is probably that, on the one hand, arsenic is highly volatile and, on the other hand, there exists a large domain of very stable glasses, which extends from 0 to 60 at.% As.

The As_2Se_3 compound crystallizes in the $P2_1/n$ monoclinic space group and is an isotype of As_2S_3. Dembovskii and Luzhnaya [9] give the lattice parameters:

$a=12.503$ Å, $b=9.890$ Å, $c=4.277$ Å

and $\alpha=90°28'$ with $Z=4$

According to Renninger and Averbach [14] the As_4Se_4 compound is an isotype of realgar, As_4S_4, and crystallizes in the monoclinic system with the lattice parameters:

$a=6.69$ Å, $b=13.86$ Å, $c=10.00$ Å and $\beta=113.2°$

Bastow and Whitfield [13] studied the structure of the As_4Se_3 dimorphic compound:

(1) The low-temperature phase is described in the orthorhombic system with the parameters:

$a=9.46$ Å, $b=7.97$ Å and $c=10.47$ Å

with $Z=4$

(2) The high-temperature phase is monoclinic with the lattice parameters:

$a=25.62$ Å, $b=6.52$ Å, $c=23.01$ Å,

$\beta=126°$ and $Z=16$

Fig. 4 shows the As–Se phase diagram, given by Myers and Felty [10].

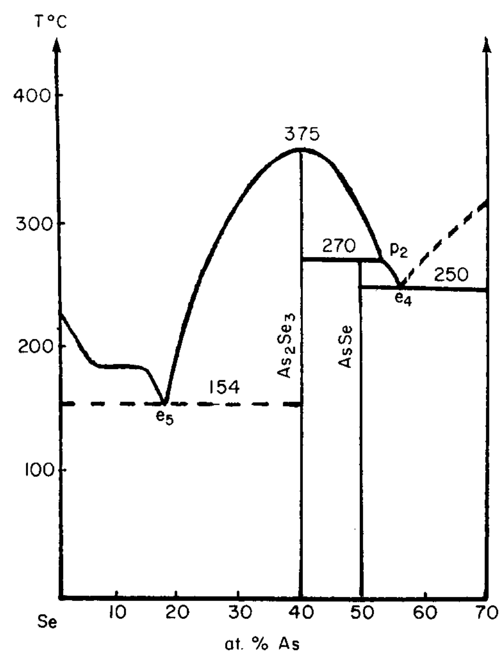

Fig. 4. Phase diagram of the As–Se binary system described by Myers and Felty [10].

4. The Cu–As–Se ternary system

4.1. Triangulation of the ternary system

Fig. 5 shows the stable domains of the different binary and ternary phases. Although the triangulation depends on the interval of temperature chosen (Fig. 6), the number of ternary phases, n, always obeys Rhines' law [15]:

$$n = b + 2t + 1$$

where b and t are the numbers of the binary and ternary phases respectively. The existence of miscibility domains, near the Cu_2Se and Cu_3As binary compounds and the Cu element, involves two phase domains, which are not represented in Fig. 6. The invariant lines defining the triangulation of the ternary system are obtained by the Guertler method [16]. The study of the different quasi-binary sections, according to Rhines [15], and common sections is necessary to design the eutectic valleys in the ternary system.

When the sections are slightly inclined to the Cu–Se binary line, the compositions along the quasi-binary sections are given by the ratio $\rho = As/(As + Se)$. On the other hand the compositions along the Cu_3AsSe_4–Se and Se–"$Cu_8As_{14}Se_{28}$" lines are given by the ratio $\rho' = Se/(Cu + As + Se)$.

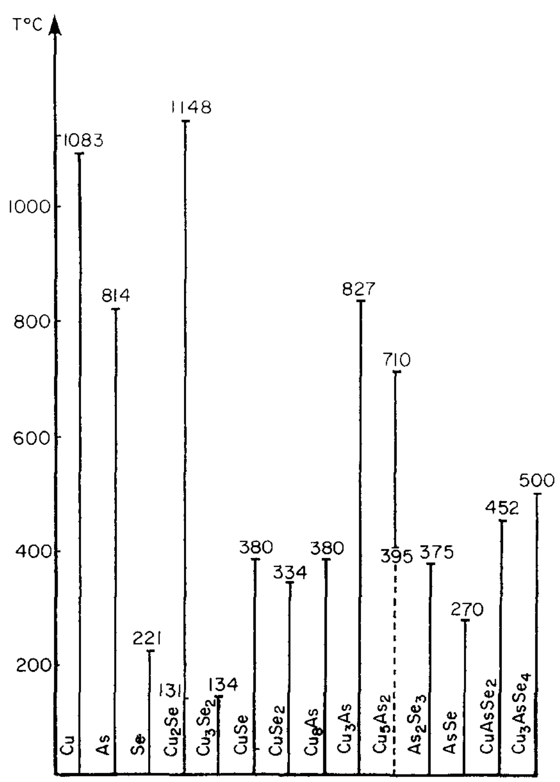

Fig. 5. Stability domain of the binary and ternary compounds versus temperature.

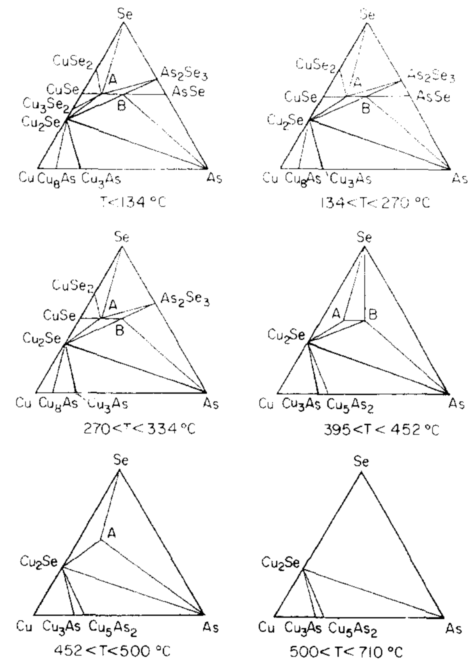

Fig. 6. Different isothermal sections of the Cu–As–Se system.

4.2. The Cu_2Se–Cu_3As quasi-binary section (Fig. 7)

This quasi-binary section joins two congruently melting compounds, Cu_2Se and Cu_3As. The X-ray diffraction patterns of alloys located along the section show a melt of the two compounds Cu_2Se and Cu_3As. This section can be treated straightforwardly: the study was performed to determine the crossing of the eutectic valley. The isothermal line at 695 °C gives the position of the pseudobinary eutectic ϵ_1, which corresponds to the ratio $\rho = 0.79$.

From both sides of the Cu_2Se–Cu_3As section, the eutectic valley decreases and meets the ternary invariants E_1 and P_1. The eutectic ϵ_1 is a saddle point. This section crosses a miscibility domain, resulting in an isothermal monotectic line at 824 °C, which is horizontal; this confirms the quasi-binary feature of this section. The liquid–liquid miscibility gap extends between the ratios $\rho_1 = 0.24$ and $\rho_2 = 0.61$. The line at 135 °C represents the phase transition of the Cu_2Se compound and can be observed along this section. However, the intensities of the endothermic peaks decrease with decreasing percentage of Cu_2Se (Table 4).

4.3. The Cu_2Se–As quasi-binary section (Fig. 8)

The Cu_2Se–As section shows an isothermal line at 135 °C, which we ascribe to the α–β Cu_2Se phase transition. One of the ternary invariants is given by an isothermal line at 676 °C, attributed to the Cu_2Se–Cu_3As–Cu_5As_2 ternary triangle. The quasi-binary eutectic ϵ_2 is situated at 720 °C with a composition of

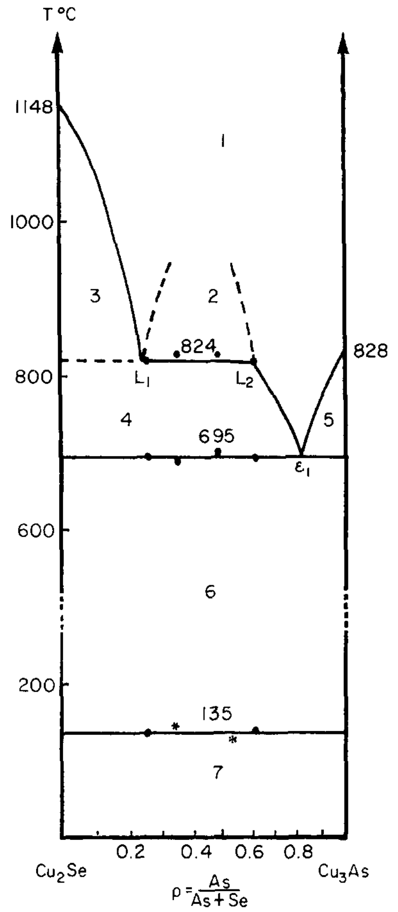

Fig. 7. Phase diagram of the Cu_2Se–Cu_3As section.

Table 4
Phase equilibria in the domains crossed by the Cu_2Se–Cu_3As section

Domain number	Phases
1	L
2	$L_1 + L_2$
3	$L + Cu_2Se\beta$
4	$L + Cu_2Se\beta$
5	$L + Cu_3As$
6	$Cu_2Se\beta + Cu_3As$
7	$Cu_2Se\alpha + Cu_3As$

$Cu_{5.5}As_{1.8}Se_{2.7}$. The $Cu_{2-x}Se$ solid solution originates from the Cu–Se binary system and extends into the ternary system up to a ratio of $\rho = 0.18$; the maximal extension of this solid solution is situated at the temperature of the quasi-binary eutectic ϵ_2.

In the triangle Cu_2Se–Cu_5As_2–As the eutectic valley decreases on one side towards the ternary invariant E_2 and on the other side, through the triangle Cu_2Se–$CuAsSe_2$–As, towards the ternary invariant P_2. The finding that eutectic ϵ_2 is a saddle point confirms the quasi-binary feature of the Cu_2Se–As section. Because of the high volatility of arsenic, the samples are no longer homogeneous beyond the ratio $\rho = 0.90$ (Table 5).

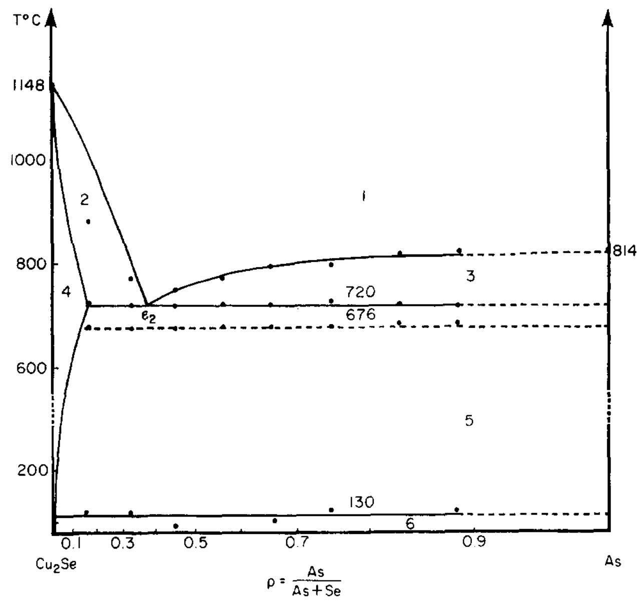

Fig. 8. Phase diagram of the Cu_2Se–As section.

Table 5
Phase equilibria in the domains crossed by the Cu_2Se–As section

Domain number	Phases
1	L
2	$L + (Cu_2Se)$
3	$L + As$
4	(Cu_2Se)
5	$Cu_2Se\beta + As$
6	$Cu_2Se\alpha + As$

4.4. The Cu_2Se–As_2Se_3 section (Fig. 9)

This section confirms the existence of the $CuAsSe_2$ ternary compound, which undergoes a peritectic decomposition of the binary type at 452 °C:

$$CuAsSe_2 \rightleftharpoons (Cu_2Se) + \text{Liq. } \pi$$

A detailed study concerning the $CuAsSe_2$ compound is under way as this compound seems to be interesting, localized at the boundary of the glassy area.

The quasi-binary eutectic ϵ_3 ($\rho = 0.39$) is an isothermal line at 360 °C and indicates that the eutectic valley passing from P_3 to P_4 crosses the Cu_2Se–As_2Se_3 section. The solid solution originating from the Cu_2Se compound extends up to $\rho = 0.13$, at 452 °C. As the Cu_2Se and As_2Se_3 compounds melt congruently and as the eutectic valley decreases from both sides of the Cu_2Se–As_2Se_3 section, the eutectic ϵ_3 is a saddle point and the section is a quasi-binary one. At 360 °C the equilibrium is given by

$$\text{Liq. } \epsilon_3 \rightleftharpoons CuAsSe_2 + As_2Se_3$$

The DTA technique does not allow us to find the isothermal line at 135 °C, given in Fig. 9 as a dotted line; the enthalpy change of the transformation of the Cu_2Se phase must be rather small. Table 6 shows the different phases at equilibrium in each domain of the section.

4.5. The Cu_2Se–"As_2Se_5" section (Fig. 10)

This section is formed by two contiguous parts: the first one, Cu_2Se–Cu_3AsSe_4, shows a quasi-binary behaviour; the second one, Cu_3AsSe_4–"As_2Se_5", is a common section in the ternary system.

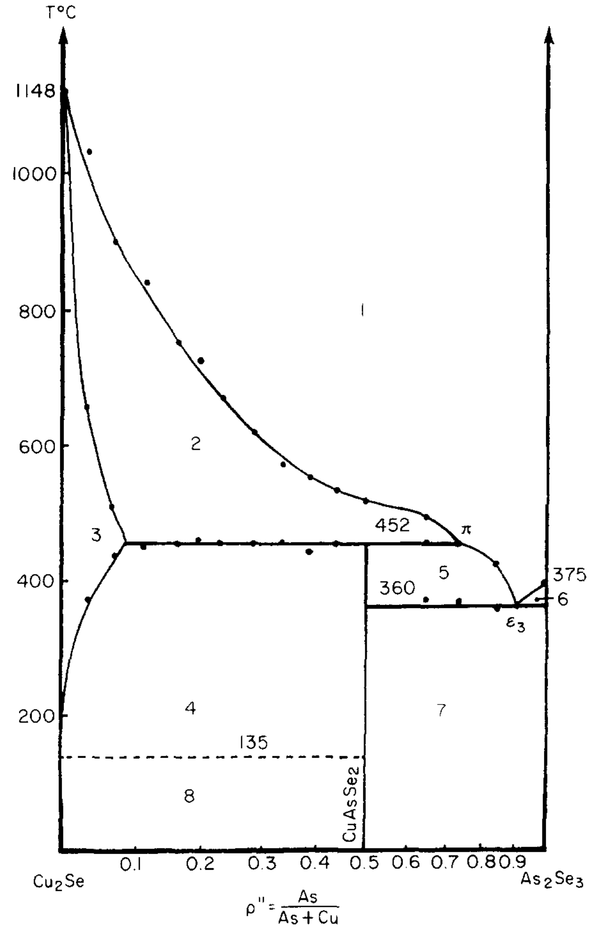

Fig. 9. Phase diagram of the Cu_2Se–As_2Se_3 section.

Table 6
Phase equilibria in the domains crossed by the Cu_2Se–As_2Se_3 section

Domain number	Phases
1	L
2	L + ($Cu_2Se\beta$)
3	(Cu_2Se)
4	($Cu_2Se\beta$) + $CuAsSe_2$
5	$CuAsSe_2$ + L
6	As_2Se_3 + L
7	$CuAsSe_2$ + As_2Se_3
8	$CuAsSe_2$ + ($Cu_2Se\alpha$)

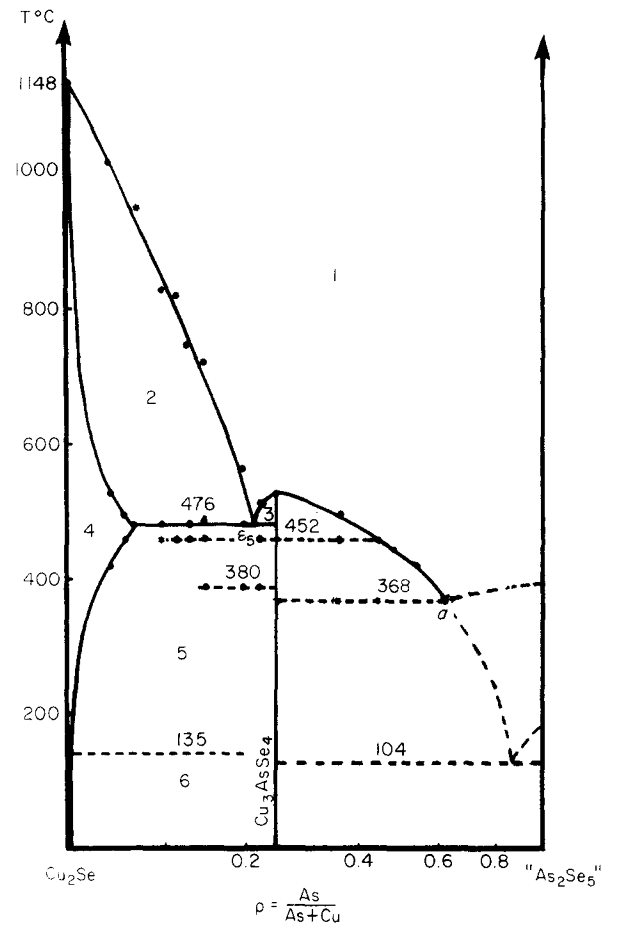

Fig. 10. Phase diagram of the Cu_2Se–"As_2Se_5" section.

Table 7
Phase equilibria in the domains crossed by the Cu_2Se–Cu_3AsSe_4 section

Number	Phases
1	L
2	L + ($Cu_2Se\beta$)
3	L + Cu_3AsSe_4
4	($Cu_2Se\beta$)
5	($Cu_2Se\beta$) + Cu_3AsSe_4
6	($Cu_2Se\alpha$) + Cu_3AsSe_4

In the quasi-binary part, the isothermal line at 452 °C, attributed to the peritectoid decomposition of $CuAsSe_2$, is still noticed because of the vicinity of the Cu_2Se–Cu_3AsSe_4 and Cu_2Se–As_2Se_3 sections. The isothermal line at 380 °C is only observed in the region rich in Cu_3AsSe_4 and is attributed to the vertical section of the invariant plane of the CuSe compound. This section is important as it shows the temperature maximum (point ϵ_5) of the eutectic valley E_4E_5 on its way down to the ternary peritectic point P_5 of the Cu_2Se–CuSe–Cu_3AsSe_4 triangle. The eutectic valley surrounds the Cu_3AsSe_4 congruent melting compound, thus limiting its crystallization area (Table 7).

In the Cu_3AsSe_4–"As_2Se_5" common section, only two isothermal lines appear. The first one is observed at the temperature of 368 °C, where the eutectic valley crosses this section (point a) on its way to the ternary eutectic point E_5 of the Cu_3AsSe_4–Se–As_2Se triangle. The second one at 452 °C shows the peritectic decomposition of the $CuAsSe_2$ compound.

4.6. The Cu_3AsSe_4–Se quasi-binary section (Fig. 11)

Many isothermal lines appear on this section. The isothermal line at 220 °C corresponds to the temperature of the quasi-binary eutectic, degenerated at the Se apex. We attribute the lines at 331 °C and 366 °C to the invariant planes of the $CuSe_2$ and CuSe binary compounds respectively. The monotectic plane at 415 °C is shown in Fig. 11 by dotted lines.

The Cu_3AsSe_4 compound and the element Se melt congruently. The ϵ_6 quasi-binary eutectic corresponds to the equilibrium:

$$\text{Liq. } \epsilon_6 \rightleftharpoons Cu_3AsSe_4 + Se$$

Thus this section is a quasi-binary one. This finding is confirmed by the fact that the isothermal line at 444 °C, corresponding to the liquid–liquid miscibility gap, is horizontal. Table 8 gives the phase equilibria.

4.7. The Cu_3AsSe_4–As_2Se_3 section (Fig. 12)

On this section a quasi-binary eutectic ϵ_4 ($\rho = 0.35$) appears at the temperature of 372 °C. The eutectic valley going from E_4 to E_5 decreases from both sides of the binary eutectic ϵ_4; this section is thus a quasi-binary one (Table 9).

The ternary eutectic E_5 of the Cu_3AsSe_4-As_2Se_3-Se triangle is found at the temperature of 104 °C and corresponds to the equilibrium:

$$\text{Liq. } E_5 \rightleftharpoons Cu_3AsSe_4 + As_2Se_3 + Se$$

Table 8
Phase equilibria in the domains crossed by the Cu_3AsSe_4–Se section

Domain number	Phases
1	L
2	$L_1 + L_2$
3	$L + Cu_3AsSe_4$
4	$L + Cu_3AsSe_4$
5	$Cu_3AsSe_4 + Se$
6	$L + Se$

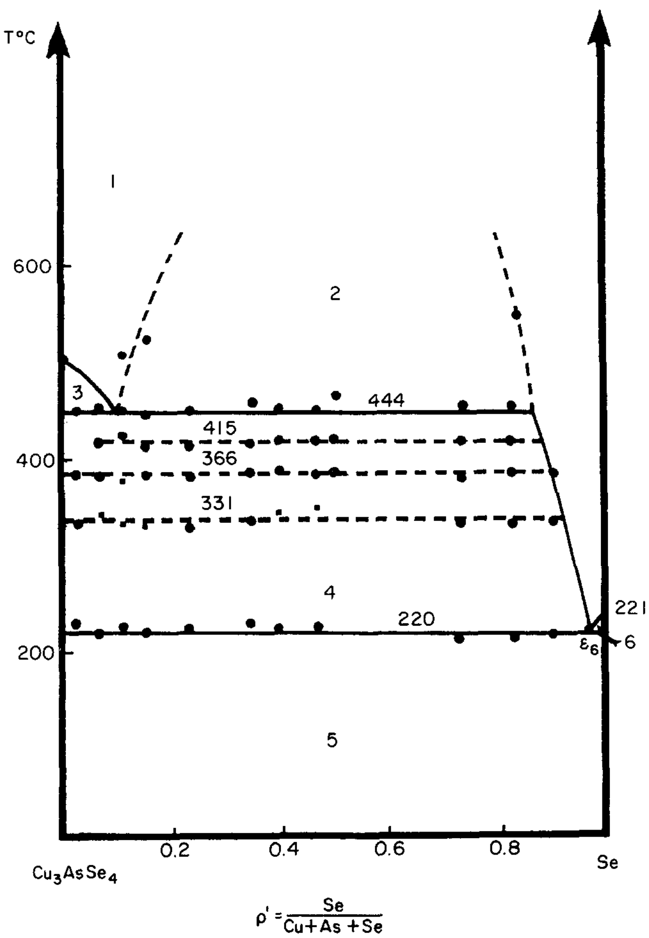

Fig. 11. Phase diagram of the Cu_3AsSe_4–Se section.

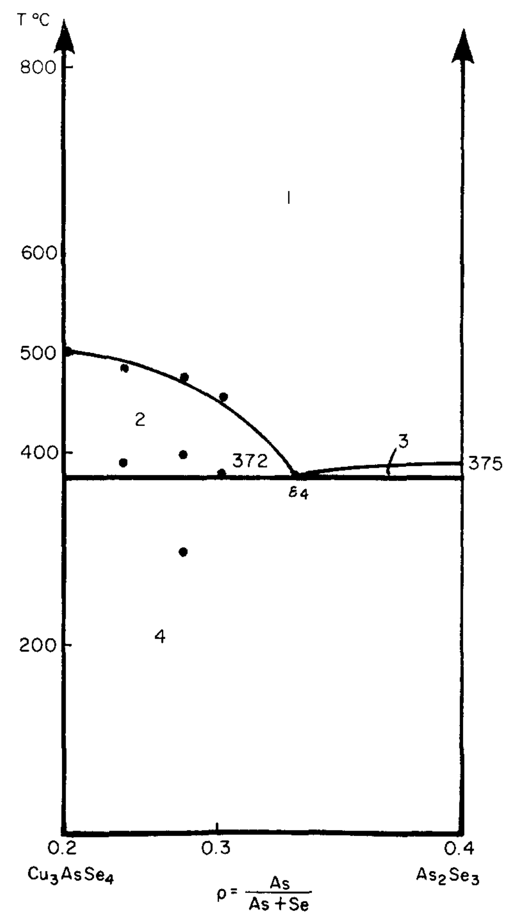

Fig. 12. Phase diagram of the Cu_3AsSe_4–As_2Se_3 section.

Table 9
Phase equilibria in the domains crossed by the Cu_3AsSe_4–As_2Se_3 section

Domain number	Phases
1	L
1	L + Cu_3AsSe_4
3	L + As_2Se_3
4	Cu_3AsSe_4 + As_2Se_3

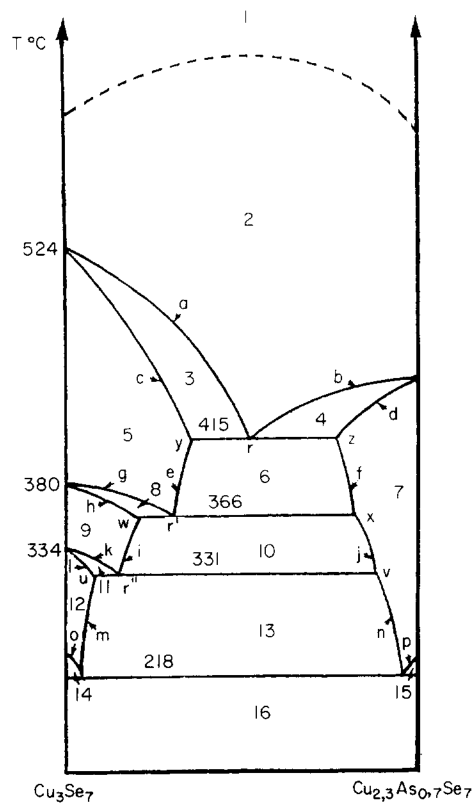

Fig. 13. Phase diagram of the section at 70 at.% Se.

The ternary eutectic E_4 of the Cu_3AsSe_4–As_2Se_3–$CuAsSe_2$ system at 330 °C gives the reaction:

$$\text{Liq. } E_4 \rightleftarrows Cu_3AsSe_4 + As_2Se_3 + CuAsSe_2$$

The quasi-binary invariant points are localized in temperature and composition. In order to confirm and to state precisely our drawing of the eutectic valleys in the ternary system we present two other common sections: the common section at 70 at.%. Se and the common section Se–"$Cu_8As_{14}Se_{28}$".

4.8. *The common section at 70 at.% Se (Fig. 13)*

To give a complete description of this section from the Cu_3Se_7 to the $Cu_{2.7}As_{0.3}Se_7$ composition, we found it necessary to associate the experimental study with the theory of the phase diagrams. The major difficulty encountered was essentially due to the great number of thermal phenomena that occurred in a small range of composition. The section crosses four invariant planes: a eutectic plane at 218 °C, two peritectic planes at 331 °C and at 366 °C corresponding to the peritectic decompositions of the compounds $CuSe_2$ and CuSe, respectively, and finally a monotectic plane at 415 °C. The section cuts:

(1) at the points u and v, the minimal tie lines originating from Cu_2Se and Cu_3AsSe_4 respectively, which go through P_6;
(2) at the point r″, the minimal tie line originating from CuSe, which goes through P_6;
(3) at the points w and x, the minimal tie lines originating from CuSe and Cu_3AsSe_4, respectively, which go through P_5:
(4) at the point r′, the minimal tie line originating from Cu_2Se, which goes through P_5;
(5) at the points y and z, the minimal tie lines originating from Cu_2Se and Cu_3AsSe_4 respectively, which go through L''_2;
(6) at the point r, the monotectic valley $L''_1L''_2$.

From each compound are originated one or several ruled surfaces, which lean on the eutectic or peritectic valleys or on the miscibility line when a ternary liquid–liquid miscibility gap exists. As the temperature decreases the section cuts the liquidus surfaces. The following pairs of curves are produced by intersection of the common section with ruled surfaces:

(1) curves a and b, when the ruled surfaces originate from the Cu_2Se–Se binary monotectic plane at 524 °C and from the Cu_3AsSe_4–Se quasi-binary monotectic plane at 444 °C respectively. The two ruled surfaces converge on the minimal tie line $L''_1L''_2$, which is merged with the eutectic valley in the ternary monotectic plane at 415 °C;
(2) curves c and d, when the ruled surfaces originate from Cu_2Se and Cu_3AsSe_4, leaning on the miscibility lines $l_2L''_2$ and $l'_2L''_2$ respectively;
(3) curves e and f, when the ruled surfaces originate from Cu_2Se and Cu_3AsSe_4, leaning on the peritectic valley L''_2P_5;
(4) curves g and h, when the ruled surfaces originate from Cu_2Se and CuSe; the two ruled surfaces lean on the peritectic valley p_3P_5;
(5) curves i and j, when the ruled surfaces originate from CuSe and Cu_3AsSe_4; these two ruled surfaces lean on the peritectic valley P_5P_6;
(6) curves l and k, when the ruled surfaces originate from $CuSe_2$ and CuSe, leaning on the peritectic valley p_4P_6;
(7) curves m and n, when the ruled surfaces originate from $CuSe_2$ and Cu_3AsSe_4, leaning on the peritectic valley P_6E_6;
(8) curves o and p, when the ruled surfaces originate from Cu_2Se and Cu_3AsSe_4; the ruled surfaces lean along the eutectic valleys e_6E_6 and ϵ_6E_6.

Table 10 shows the different phases at equilibrium in each domain of the section.

4.9. *The Se–"$Cu_8As_{14}Se_{28}$" common section (Fig. 14)*

In the part of this section rich in Se an isothermal line appears at 104 °C and corresponds to the ternary invariant point E_5 of the ternary triangle Cu_3AsSe_4–Se–As_2Se_3. The isothermal line at 218 °C corresponds to the ternary eutectic which is degenerated at the Se apex (point b). On the other hand, at 368 °C the eutectic valley ϵ_4E_5 crosses the section at the point a and joins the ternary eutectic point E_5. This section cuts a liquid–liquid miscibility gap, which gives rise to a non-horizontal monotectic line; this confirms that the section is not a quasi-binary one. As the liquid–liquid miscibility zone extends into the Cu–As–Se ternary system the temperature of this monotectic line decreases.

5. The liquid–liquid miscibility gaps

5.1. *The two-liquid miscibility gap originating from the Cu–Cu_2Se binary system*

The miscibility gap originates from the binary monotectic system at 1107 °C. As it is not crossed by any eutectic valley, this miscibility gap is simple. At 824 °C the liquid–liquid miscibility gap intersects the Cu_2Se–Cu_3As section and gives rise to an isothermal horizontal line, which confirms the quasi-binary feature of the Cu_2Se–Cu_3As section. At about 680 °C, the boundary curve presents a minimum critical point C_m, which is located inside the Cu_2Se–Cu_3As–As triangle.

Table 10
Phase equilibria in the domains crossed by the section at 70 at.% Se

Domain number	Phases
1	L
2	L_1+L_2
3	$L_1+L_2+Cu_2Se$
4	$L_1+L_2+Cu_3AsSe_4$
5	$L+Cu_2Se$
6	$L+Cu_2Se+Cu_3AsSe_4$
7	$L+Cu_3AsSe_4$
8	$L+Cu_2Se+CuSe$
9	$L+CuSe$
10	$L+CuSe+Cu_3AsSe_4$
11	$L+CuSe+CuSe_2$
12	$L+CuSe_2$
13	$L+CuSe_2+Cu_3AsSe_4$
14	$L+CuSe_2+Se$
15	$L+Cu_3AsSe_4+Se$
16	$CuSe_2+Cu_3AsSe_4+Se$

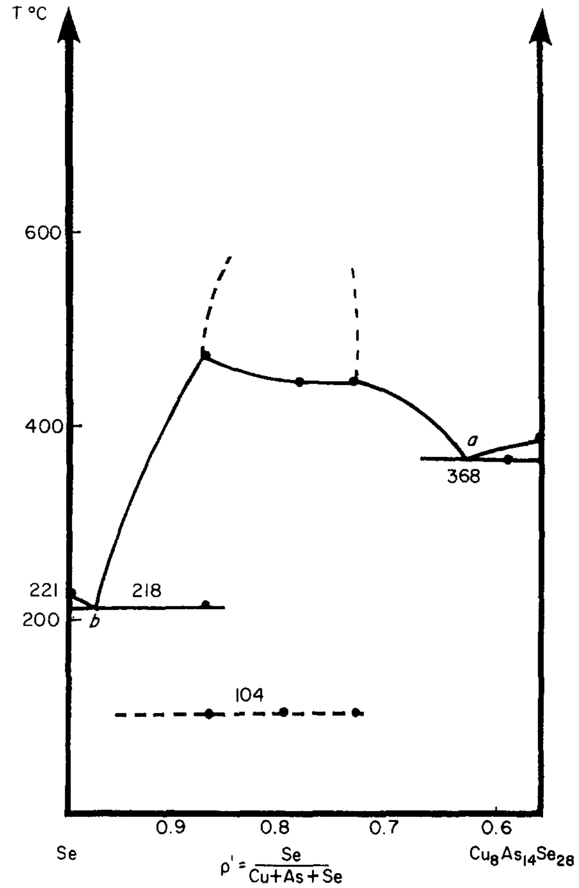

Fig. 14. Phase diagram of the Se–"$Cu_8As_{14}Se_{28}$" section.

This miscibility gap is visible to the naked eye. Samples heated up to 1180 °C and then quenched in cold water show two parts: the outside is orange-coloured and the inside grey-coloured. The existence of this miscibility gap was confirmed by observation using a metallographic microscope (Fig. 15). The orange melt corresponds to the phase rich in Cu, and the grey melt is attributed to the phase rich in Cu_2Se.

5.2. *The two-liquid miscibility gap originating from the Cu_2Se–Se binary system*

The miscibility gap, originating from the Cu_2Se–Se system, largely extends into the ternary system. From the monotectic line localized at 524 °C, the surface of the miscibility gap successively crosses the eutectic valley ϵ_5E_6 with a monotectic line at 415 °C and the Cu_3AsSe_4–Se quasi-binary system where the monotectic line reaches a maximal temperature of 444 °C. The extreme boundary of the miscibility gap is close to the eutectic valley E_4E_5, in the triangle Cu_3AsSe_4–As_2Se_3–Se, and shows a minimum critical point C'_m at about 350 °C.

When the eutectic valley ϵ_5E_6, along which the Cu_3AsSe_4 and Cu_2Se congruently melting compounds simultaneously crystallize, crosses the liquid miscibility

Fig. 15. Micrograph of the liquid–liquid miscibility gap originating from the Cu–Cu_2Se binary system (magnification: 800×).

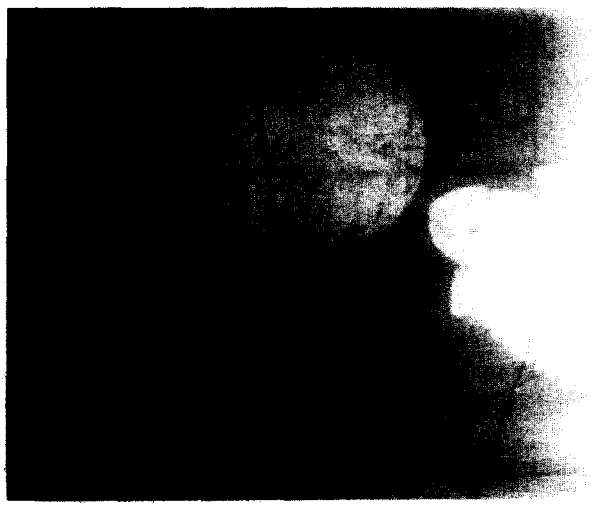

Fig. 16. Micrograph of the liquid–liquid miscibility gap originating from the Cu_2Se–Se binary system (magnification: 800×).

gap, a first-class monotectic equilibrium is expressed by the reaction at 415 °C:

$$L''_1 \rightleftharpoons L''_2 + Cu_2Se + Cu_3AsSe_4$$

The existence of this miscibility gap was confirmed by observation using a metallographic microscope (Fig. 16). Fig. 17 shows that this equilibrium is in agreement with its geometrical position, inside the triangle L''_2–Cu_2Se–Cu_3AsSe_4. At higher temperatures, this equilibrium is preceeded, by two series of monovariant equilibria:

(1) the equilibrium

$$L \rightleftharpoons Cu_2Se + Cu_3AsSe_4$$

which is found along the eutectic valley originating from the quasi-binary eutectic ϵ_5 of the Cu_2Se–Cu_3AsSe_4 section;

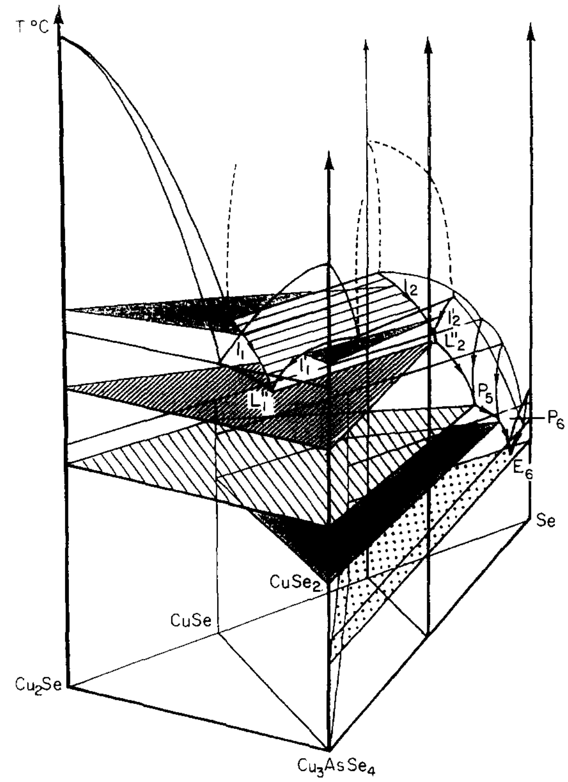

Fig. 17. Extension, in the ternary system, of the two liquid–liquid miscibility gaps originating from the Cu–Se binary system.

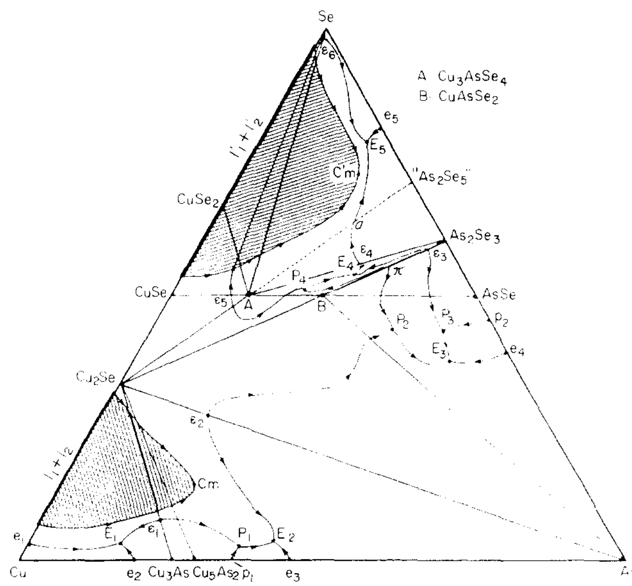

Fig. 18. Phase diagram of the Cu–As–Se ternary system.

(2) the monovariant equilibria

$$l_1 \rightleftharpoons l_2 + Cu_2Se$$

and

$$l'_1 \rightleftharpoons l'_2 + Cu_3AsSe_4$$

which originate from the binary miscibility gaps and exist down to the temperature of the ternary monotectic equilibrium. The tie triangles $Cu_2Sel_1l_2$

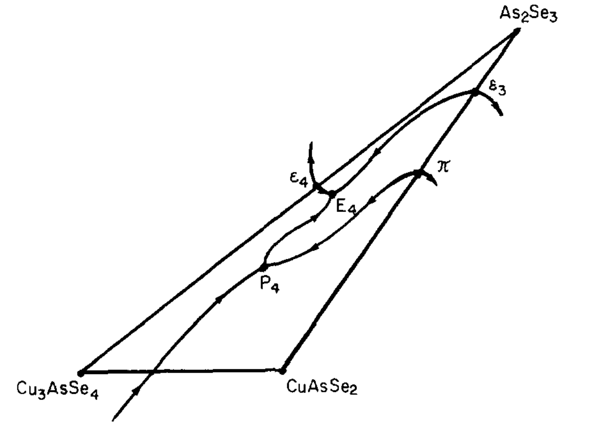

Fig. 19. Drawing of the eutectic valleys in the triangle Cu_3AsSe_4–$CuAsSe_2$–As_2Se_3.

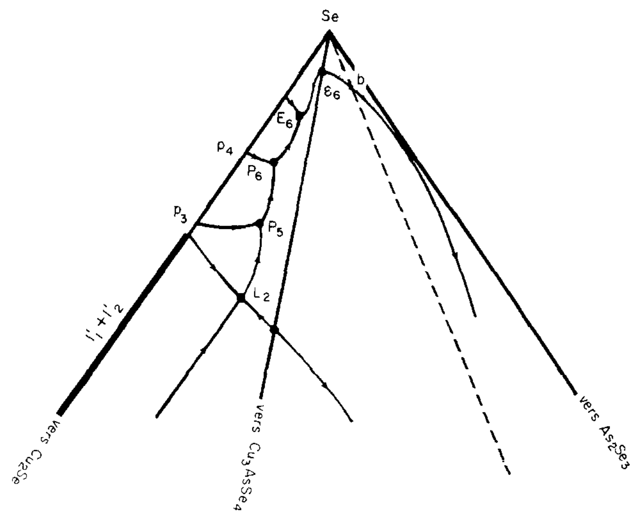

Fig. 20. Drawing of the eutectic valleys in the triangle Cu_2Se–Cu_3AsSe_4–Se.

and $Cu_3AsSe_4l'_1l'_2$ are shown on the projection of the composition triangle (Fig. 17). They describe the crystallization surfaces of the Cu_2Se and Cu_3AsSe_4 compounds, respectively.

The eutectic valley, which is the continuation of the ternary monotectic equilibrium, starts at the point L''_2 and ends at the ternary eutectic point E_6. The three-dimensional Fig. 17 shows the lower limit plane of the miscibility gap and the eutectic and monotectic invariant planes inside the Cu_2Se–Cu_3AsSe_4–Se triangle.

6. The evolution of the solid–liquid equilibria (Fig. 18)

The eutectic valley originating from ϵ_1, at 695 °C, meets two other valleys at the point E_1. The first one of these latter valleys originates from the eutectic point e_1 of the Cu–Se system at 1063 °C, and the second one originates from the eutectic point e_2 of the Cu–As system at 685 °C. The equilibrium at 680 °C is written:

$$\text{Liq. } E_1 \rightleftharpoons Cu + Cu_3As + Cu_2Se$$

The Cu_2Se–Cu_3As–As triangle is subdivided into two secondary triangles. The Cu_2Se–Cu_3As–Cu_5As_2 triangle admits a ternary peritectic point P_1 with the equilibrium at 676 °C:

$$\text{Liq. } P_1 + Cu_3As \rightleftharpoons Cu_5As_2 + Cu_2Se$$

The eutectic valley originating from ϵ_2 at 720 °C meets at E_2 two valleys, which come from the peritectic point P_1 and from the binary eutectic point e_3. The eutectic point E_2 of the Cu_2Se–Cu_5As_2–As triangle corresponds to the equilibrium at 592 °C:

$$\text{Liq. } E_2 \rightleftharpoons Cu_2Se + Cu_5As_2 + As$$

The two valleys originating from the quasi-binary peritectic point π at 415 °C and from the pseudo-binary eutectic point ϵ_2 at 720 °C meet at the peritectic point P_2, where they give a peritectic reaction at 371 °C:

$$\text{Liq. } P_2 + Cu_2Se \rightleftharpoons CuAsSe_2 + As$$

The two valleys originating from the peritectic point P_2 and from the quasi-binary eutectic point ϵ_3 at 360 °C decrease and join each other at the point P_3, where they give, at 223 °C, a quasi-peritectic equilibrium:

$$\text{Liq. } P_3 + As_2Se_3 \rightleftharpoons CuAsSe_2 + AsSe$$

The two valleys originating from the binary peritectic point p_2 at 270 °C and from the binary eutectic point e_4 at 250 °C converge and meet a third valley, originating from P_3 at the ternary eutectic point E_3. The ternary equilibrium at 195 °C is given by the equation:

$$\text{Liq. } E_3 \rightleftharpoons CuAsSe_2 + AsSe + As$$

The two valleys originating from the quasi-binary point ϵ_5 at 476 °C and from the quasi-binary point π at 452 °C join each other at the peritectic point P_4 at 351 °C (Fig. 19). At this point we obtain a quasi-peritectic reaction:

$$\text{Liq. } P_4 + Cu_2Se \rightleftharpoons Cu_3AsSe_4 + CuAsSe_2$$

The two valleys originating from the quasi-binary eutectic points ϵ_3 and ϵ_4 at 360 °C and 372 °C, respectively, meet at the point E_4, at 330 °C, the valley originating from the peritectic point P_4. The ternary equilibrium is:

$$\text{Liq. } E_4 \rightleftharpoons Cu_3AsSe_4 + CuAsSe_2 + As_2Se_3$$

The two valleys originating from the quasi-binary eutectic points ϵ_4 and ϵ_6 at 372 °C and 220 °C, respectively join at the point E_5, at 104 °C, the eutectic valley which comes from the binary eutectic point e_5. The ternary equilibrium is given by:

$$\text{Liq. } E_5 \rightleftharpoons Cu_3AsSe_4 + As_2Se_3 + Se$$

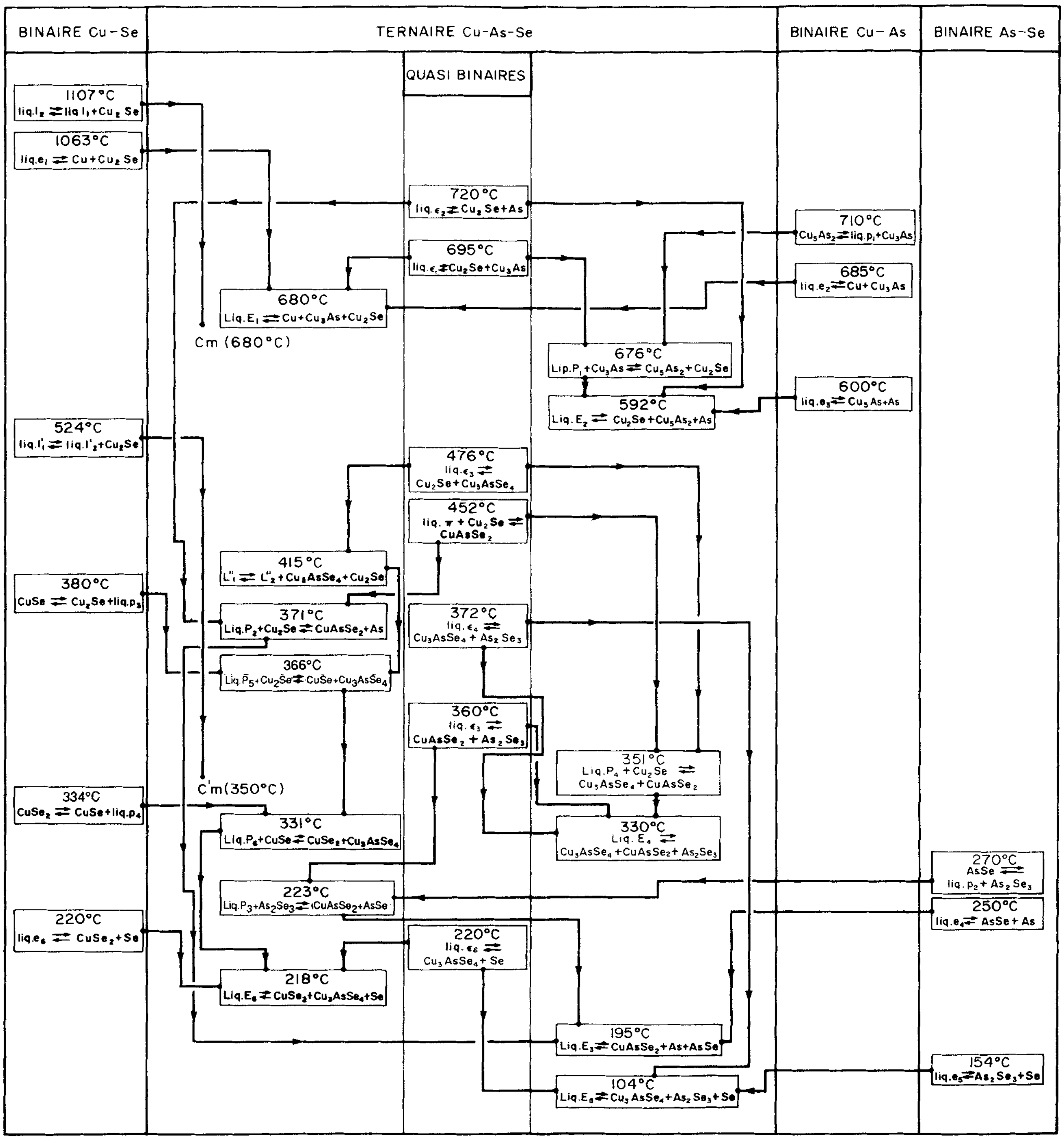

Fig. 21. Liquid–solid equilibria in the Cu–As–Se ternary system.

When the eutectic valley originating from the quasi-binary eutectic point ϵ_5 crosses the miscibility gap which comes from the Cu_2Se–Se binary system, a first-class ternary monotectic equilibrium is established at 415 °C:

$$L''_1 \rightleftharpoons L''_2 + Cu_3AsSe_4 + Cu_2Se$$

As the temperature decreases this eutectic valley follows the path $L''_1L''_2$ to E_6 through the peritectic points P_5 and P_6 (Fig. 20). At P_5, this valley is joined by the valley originating from the binary peritectic point p_3. At 366 °C the equilibrium is:

$$\text{Liq. } P_5 + Cu_2Se \rightleftharpoons CuSe + Cu_3AsSe_4$$

At P_6 the valley is joined by the one coming from the binary peritectic point p_4. At 331 °C the equilibrium is given by:

$$\text{Liq. } P_6 + CuSe \rightleftharpoons CuSe_2 + Cu_3AsSe_4$$

The three valleys originating from the two eutectic points e_6 and ϵ_6 and from the peritectic point P_6 intersect each other at the eutectic point E_6. At 218 °C the equilibrium is:

$$\text{Liq. } E_6 \rightleftharpoons CuSe_2 + Cu_3AsSe_4 + Se$$

Fig. 21 shows the evolution of the solid–liquid equilibria in the Cu–As–Se ternary system.

7. Conclusion

The Cu–As–Se system is characterized by the presence of two ternary compounds. The first one, Cu_3AsSe_4, congruently melts at the temperature of 500 °C; the second one, $CuAsSe_2$, undergoes a peritectic decomposition of the binary type at 452 °C:

$$CuAsSe_2 \rightleftharpoons \text{Liq. } \pi + Cu_2Se$$

The main triangle is subdivided into 12 secondary triangles. The ternary invariants, among which we observed six quasi-peritectic points, are localized in composition and temperature. The crystallization domains of the compounds are delimited. The ternary invariants are principally found in three regions of the ternary system: the first area is close to the compound Cu_3As, the second one is found in the area near the compound As_2Se_3, and the third one near the Se apex. As the crystallization area of arsenic is very large, the valleys are gathered in the regions rich in Cu_3As and As_2Se_3.

Two ternary liquid–liquid miscibility gaps are identified. The first one, which is localized in the region rich in Cu, is not crossed by any eutectic valley. On the other hand the second one, which is more extended, is crossed by a eutectic valley and gives a first-class monotectic equilibrium at 415 °C:

$$L''_1 \rightleftharpoons L''_2 + Cu_3AsSe_4 + Cu_2Se$$

During this study a large glassy domain originating from the As–Se binary system was bounded. It coincides with the area, near As_2Se_3, where many ternary invariant points are concentrated. The vitreous domain overlaps a small part of the liquid–liquid miscibility gap which originates from the Cu_2Se–Se binary system and gives phase-separated glasses.

References

[1] K.S. Liang, A. Bienenstock and C.W. Bates, *Phys. Rev. B, 10* (1974) 1528–1538.

[2] S.H. Hunter, Stanford Synchrotron Radiation Project Report no 77/04, Stanford University, Stanford, CA, 1977.

[3] W. Hume-Rothery and J. Burns, *Phil. Mag., 2* (1957) 1177–1196.

[4] R.D. Heyding and G.J.G. Despault, *Can. J. Chem., 38* (1960) 2477–2481.

[5] K. Schubert, H. Breimer, W. Burkhardt, E. Günzel, R. Haufler, H.L. Lukas, H. Vetter, J. Wegst and M. Wilkens, *Naturwiss., 44* (1957) 229–230.

[6] D.T. Hawkins, *Metals Handbook*, Vol. 8, American Society for Metals, Metals Park, OH, 1973.

[7] K. Friedrich and A. Leroux, *Metallurgie, 5* (1908) 355–357.

[8] R.D. Heyding, *Can. J. Chem., 44* (1966) 1233–1236.

[9] S.A. Dembovskii and N.P. Luzhnaya, *Zh. Neorg. Khim., 9* (1964) 660–664.

[10] B.M. Myers and F.J. Felty, *Mater. Res. Bull., 2* (1967) 535–546.

[11] R. Blachnik, A. Hoppe and U. Wickel, *Z. Anorg. Allg. Chem., 463* (1980) 78–90.

[12] J.-C. Rouland, Thèse de doctorat ès sciences, Université de Paris XI, Orsay, France, 1983.

[13] T.J. Bastow and H.J. Whitfield, *J. Chem. Soc. Dalton Trans., 10* (1977) 959–961.

[14] A.L. Renninger and B.L. Averbach, *Acta Crystallogr., B29* (1973) 1583–1589.

[15] F.N. Rhines, *Phase Diagrams in Metallurgy*, McGraw-Hill, New York, 1956.

[16] W. Guertler, *Met. Erz., 85* (1920) 192.